Flow Imaging

16

John N. Oshinski, Anurag Sahu, and Gregory R. Hartlage

Abstract

Phase-Contrast Magnetic Resonance (*PCMR*) is a technique used to quantitatively measure blood velocity and determine blood flow. In the first section, the technical aspects of the technique are described including the basic physics covering the generation of the phase-based velocity measurements, the specific implementation of the technique in pulse sequences, and MR parameters specific to PCMR. Advanced acquisition methods such as real-time imaging, tissue phase mapping, and 4D PCMR are described, as well as effects of parameter choices on temporal and spatial resolution. The analysis of the PCMR velocity images is explained, specifically highlighting physiologically relevant velocity and flow metrics that can be calculated from the PCMR measurements. In the second section, the clinical applications of PCMR are surveyed, concentrating on the information PCMR can provide as a complementary hemodynamic assessment of systolic and diastolic function to aide both diagnosis and prognosis in patients with cardiovascular disease. Disease conditions highlighted include myocardial disease, valve disease, and vascular disease. Special emphasis is given to congenital heart disease, where a significant number of PCMR applications have been developed.

Keywords

Blood flow • Velocity • Hemodynamics • Phase-contrast

Introduction

Magnetic Resonance Imaging (MRI) can be used to quantitatively measure blood velocity and determine flow [1]. The most widely used technique to quantify blood flow is *Phase-Contrast Magnetic Resonance* (*PCMR*), although other names for this technique exist including; phase velocity mapping, phase velocity encoding, quantitative flow imaging, etc. Other MRI-based techniques to quantify velocity flow include methods to label blood (similar to what is done in tagging), but these techniques are infrequently used [2].

This chapter is divided into two major sections, one section on the technical aspects of PCMR including physics and implementation of PCMR, and a second section on clinical applications of PCMR. The technical methodology section covers: (1) the basic physics of the generation of the phase-based velocity measurements, (2) the implementation of the technique in MR pulse sequences and advanced acquisition methods, (3) the analysis of velocity images and some of the important metrics that can be calculated from the velocity and flow measurements. The clinical application section

J.N. Oshinski, PhD (✉)
Radiology and Imaging Sciences, Emory University School of Medicine, Atlanta, GA, USA
e-mail: jnoshin@emory.edu

A. Sahu, MD
Division of Cardiology, Emory University Hospital, Atlanta, GA, USA
e-mail: Anurag.sahu@emory.edu

G.R. Hartlage, MD
Division of Cardiology, Department of Internal Medicine, Emory University, Atlanta, GA, USA
e-mail: ghartla@emory.edu

M.A. Syed et al. (eds.), *Basic Principles of Cardiovascular MRI: Physics and Imaging Technique*,
DOI 10.1007/978-3-319-22141-0_16

covers PCMR in the setting of: (1) myocardial disease, (2) valve disease, and (3) vascular disease, and (4) congenital heart disease.

The Physics of Phase Velocity Measurements

The MR signal results from a rotating magnetization vector that creates a time-varying signal in the radiofrequency (RF) receiver coils that can be measured. The vast majority of MR images are displayed as a measure of the magnitude of the vector from each spatially localized voxel. However, since the signal is time-varying, it has both a magnitude and a phase. The phase difference between two signals can be thought of as a time shift in the signals (Fig. 16.1a). PCMR works by imparting a different phase value to flowing tissue versus static tissue, thereby generating a phase shift between the two signals.

PCMR imparts this phase shift by using a bipolar magnetic field gradient during the signal acquisition. A magnetic field gradient is a linear variation of the main magnetic field in a single direction. The gradient is controlled by a set of electromagnets separate from the main magnetic field. Gradients are characterized by the time they are on (t), the direction of the variation (x, y, or z) and the value representing the slope of the field versus distance (G). The gradient $G_z(t)$ is a gradient with a positive slope value of G in the z-direction for a time t. A bipolar gradient is a gradient that is on for the same amount of time (t) in the positive (G) and negative (−G) directions (i.e., first moment = 0), Fig. 16.1b. When a bipolar gradient is applied in the direction blood is flowing, the blood will have a phase shift proportional to its motion over the time the gradient is applied. This bipolar gradient has no effect on static tissue, but imparts a phase shift to moving blood that is proportional to its velocity.

If one ignores higher order motion terms such as acceleration, the imparted phase shift is proportional to the blood velocity to within a constant. By acquiring a phase image with a bipolar gradient (velocity-encoded image) and reference phase image (velocity-compensated image) and subtracting them, the majority of the background phase shift can be removed from the images. The value which relates the measured phase shift after subtraction to the velocity is called the velocity encoding (VENC) value, and is related to the strength and duration of the applied gradients. The formula for the relationship is shown in Eq. 16.1.

$$f_z = g\int G_z(t)\, r_z(t)\, dt \qquad (16.1)$$

This is the generalized equation for phase shift. If G_z is a known bipolar gradient waveform (area under curve = 0), and we assume position of spins is: $r_z(t) = r_0 + v_z t$, the velocity can be determined within a constant. Velocity encoded and non-encoded images are acquired and subtracted to remove much of the residual background phase constant. The velocity encoding value (VENC) is the proportionality constant between velocity and phase that takes into account gradient strength and durations.

An example PCMR image after subtraction along with a corresponding magnitude image from a transverse slice through the ascending aorta at peak systole is shown in Fig. 16.2. The intensity values in the phase images are directly proportional to the velocity of spins within the voxel in the direction of the velocity encoding on a pixel-by-pixel basis. In a PCMR image, mid-grey level represents static tissue, bright signal represents flow toward the head, and the dark signal represents flow toward the feet.

Implementation of PCMR

In the previous section, we presented an overview of how PCMR works to measure velocity. In the following section, we will present few details on the implementation of PCMR and how its implementation may affect clinical measurements.

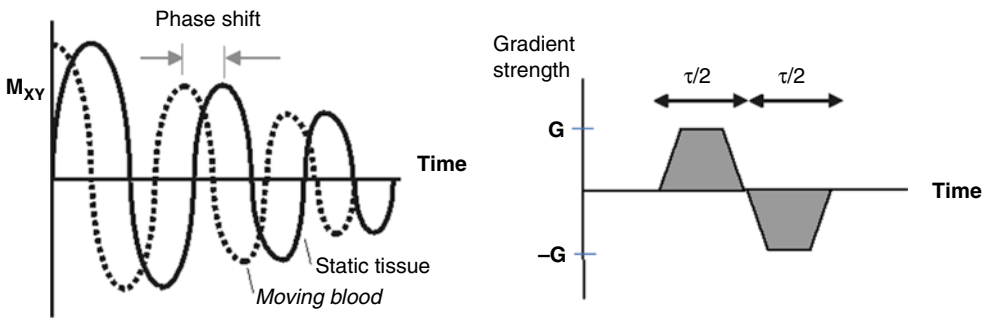

Fig. 16.1 A phase shift of the MR signal relative to static tissue is imparted to moving tissue (**a**, *left*) when a bipolar gradient is applied during signal acquisition (**b**, *right*). The phase shift can be thought of as a time shift between the signal from the static and moving spins. A bipolar gradient is a gradient that has positive and negative components with the same area

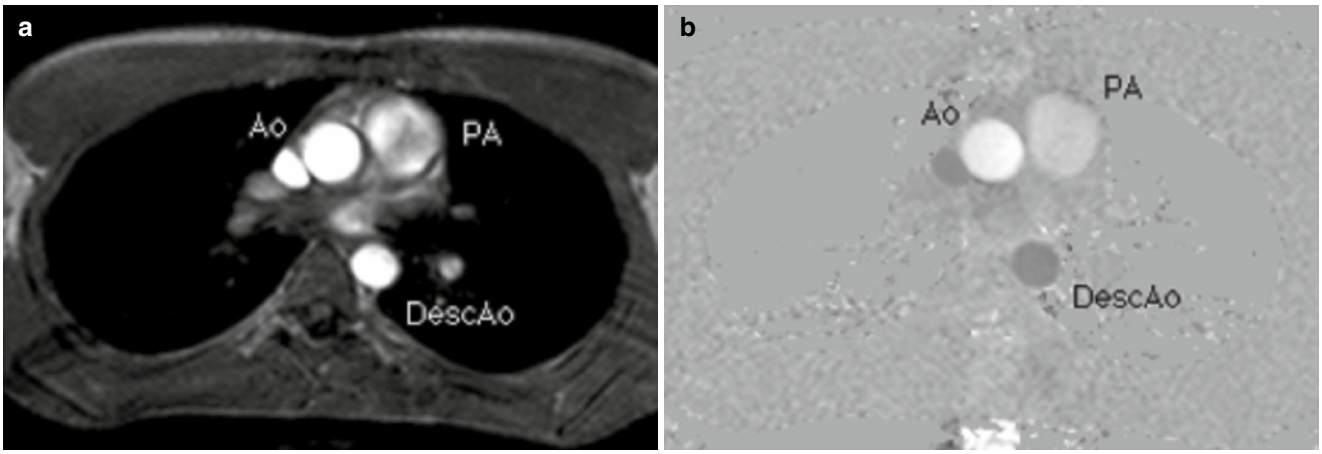

Fig. 16.2 Magnitude (*left*) and phase (*right*) images from a transverse slice through the chest just superior to the aortic valve at peak systole. Velocity is encoded in the foot-to-head direction. In the phase image the ascending aorta (*Ao*) has bright signal, indicating flow toward the head. The descending aorta (*DescAo*) is *dark*, indicating flow toward the feet. The signal intensity directly represents velocity on a pixel-by-pixel basis. The Pulmonary Artery (*PA*) velocity is lower as the area is higher in the slice location. A region of interest (ROI) is shown around the aorta to indicate the area over which to sum velocity measurements in order to get flow values

PCMR Pulse Sequences

The majority of implementations of PCMR require the use a rapid, low flip angle, gradient echo sequence. The sequence employs a short repetition time (TR) and a short echo time (TE), which minimizes de-phasing due to the presence of complex flow and increases temporal resolution when cardiac gating is used [3]. The lower flip angle reduces radiofrequency energy deposition and keeps TE as short as possible. In many applications where flow measurements are made in or near the heart, respiratory compensation is required to reduce blurring and ghosting in the images. In order to reduce acquisition time and complete the acquisition in a breath hold, segmented acquisitions strategies are often employed in which several lines of k-space are acquired for each cardiac phase. The larger the number of k-space lines that are acquired per cardiac phase, the shorter the overall acquisition time (Fig. 16.3). The penalty for the shorter overall acquisition time is a longer temporal acquisition window (reducing the true temporal resolution). Variations on this pulse sequence include the use of echo-planar techniques [4], spiral readouts strategies [5], and steady state free procession (SSFP) [6].

Cardiac Gating and Temporal Resolution

In most clinical applications of PCMR, cardiac gating is required so that multiple images at equally spaced time points over the cardiac cycle can be generated and displayed. The gating will allow generation of time versus velocity or time versus flow curves over the cardiac cycle. Prospective cardiac gating means that when the R-wave is detected, a

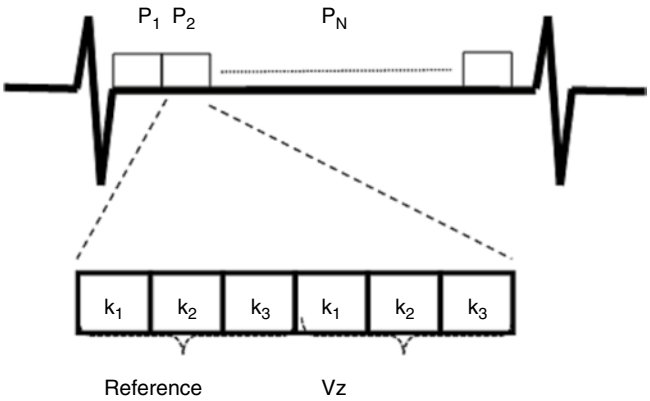

Fig. 16.3 Example of k-space segmentation in PCMR. In the diagram, 3 k-space lines (k_1, k_2, k_3) are acquired per cardiac phase ($P_1 \ldots P_N$). Because reference (non-encoded) and velocity encoded (Vz) images are acquired, the temporal window is increased and effective temporal resolution in decreased. If more lines are acquired per cardiac phase temporal resolution will decrease (lower number of true cardiac phases), but the scan duration will decrease

sequence is run over a specific time, usually ~90 % of the estimated cardiac cycle. When the next R-wave is detected, the sequence is run again with a new set of phase encoding values, and so on until the entire imaging sequence is complete. Retrospective cardiac gating acquires data continuously and keeps track of the position of the R-wave in relation to the k-space data [7]. When the acquisition is completed, data is binned into temporal phases in relation to the R-wave for reconstruction. The advantage of retrospective gating is that the entire cardiac cycle is reconstructed, prospective gating will miss ~10 % of end-diastole. Retrospective gating also allows for nearly arbitrary reconstruction of the number of phases, however, temporal smoothing occurs during

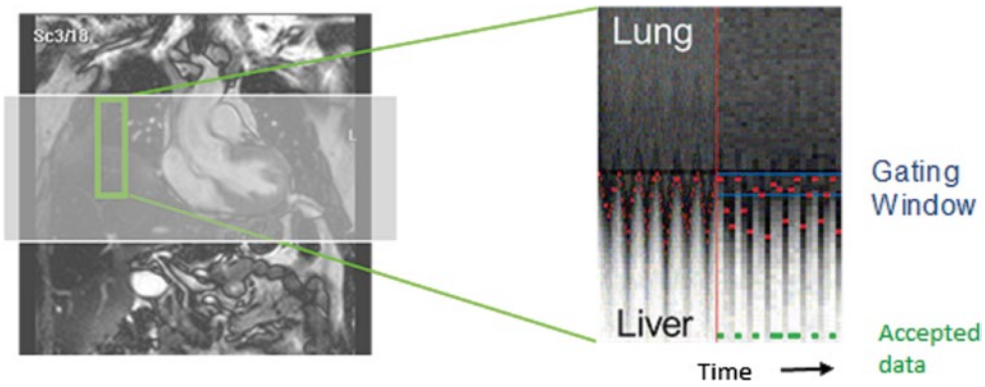

Fig. 16.4 Schematic illustrating navigator echo gating. Signal from a small region that contains the diaphragm is acquired every heart beat (or more often). The motion of the interface over time represents respiratory motion. The user may set the gating window to accept data from a certain portion of the cardiac cycle

reconstruction. The true temporal resolution of a PCMR scan can be determined by multiplying the TR by the number of segments acquired and by two (for velocity encoded and non-encoded image segments) (Fig. 16.3).

Spatial Resolution

The phase measurement from a voxel is the average phase over the entire voxel. If the pixel contains a mixture of static tissue and moving tissue, the velocity will reflect this average phase value. For flow measurements integrated over the entire vessel area this averaging has little effect on accuracy until there are less than approximately four pixels across the vessel diameter [8]. However, for estimating maximum velocity for pressure gradient calculations, or determining the velocity gradient near the wall for estimating wall shear stress, higher spatial resolution is required [9]. As with any MR sequence, increasing temporal resolution generally will increase acquisition time, decrease signal-to-noise ratio, or decrease spatial resolution.

Respiratory Compensation

As mentioned previously, in most cardiovascular applications, PCMR is executed in a breath hold to mitigate effects of respiratory motion. However, in some applications, either high spatial resolution is required, the patient cannot execute the breath hold, or a 3D volume needs to be covered. In these cases, the scan time exceeds the patient's breath hold duration capacity. Multiple signal averages can be acquired, but this often produces unacceptable image quality results and long scan times. In these cases, a navigator echo respiratory gating scheme can be employed. The navigator echo is a localized excitation beam that produces one-dimensional, time-dependent images. The beam is usually positioned over the right hemi-diaphragm and monitors the respiratory position of the diaphragm. The beam is usually executed at the beginning of the cardiac cycle and a decision is made whether the diaphragm position is within a user-defined respiratory gating window. If so, the data is used for image reconstruction, if not it is rejected and the k-space line is re-acquired (Fig. 16.4). There are multiple ways to implement navigator echo gating schemes and the gating can be done retrospectively or prospectively. The major applications of navigator echo gated PCMR are in time-resolved 3D imaging (so called 4D PCMR) [10], or in applications that require high spatial resolution such as coronary artery flow measurements [11].

Velocity Encoding Direction

The velocity encoding direction is independent of the slice orientation. Therefore, the velocity of blood (or tissue) can be encoded through the slice, or the velocity in either of the in-plane directions can be encoded. The direction of encoding can be set in the protocol which changes the direction of the bipolar velocity encoding gradient. Note that the velocity encoded in the image phase is the projection (or dot product) of the velocity vector in the direction of the encoding gradient. For example, if the PCMR image slice is off by 30° perpendicular to the velocity direction, then the displayed velocity will be the true velocity multiplied by *cosine* (*30°*), or 0.87, resulting in a velocity error of ~13 % from the true value.

Here it is important to understand the difference between velocity and flow. Velocity is the time-rate of change of position in a specific direction of fluid and has the units of length/time (i.e. cm/s). Flow is the rate of volume flux of fluid through a region per unit time and has the units of volume/time (i.e., milliliters/s). Flow requires velocity measurements to be integrated over a cross-sectional area. Therefore, flow can only be determined with through-plane velocity encoding, when estimating peak velocities, care must be taken to align the slice perpendicular to the velocity direction. Flow measurements are less susceptible to this issue as the increase in the vessel area compensates for the decrease in the value of the velocity vector due to misalignment.

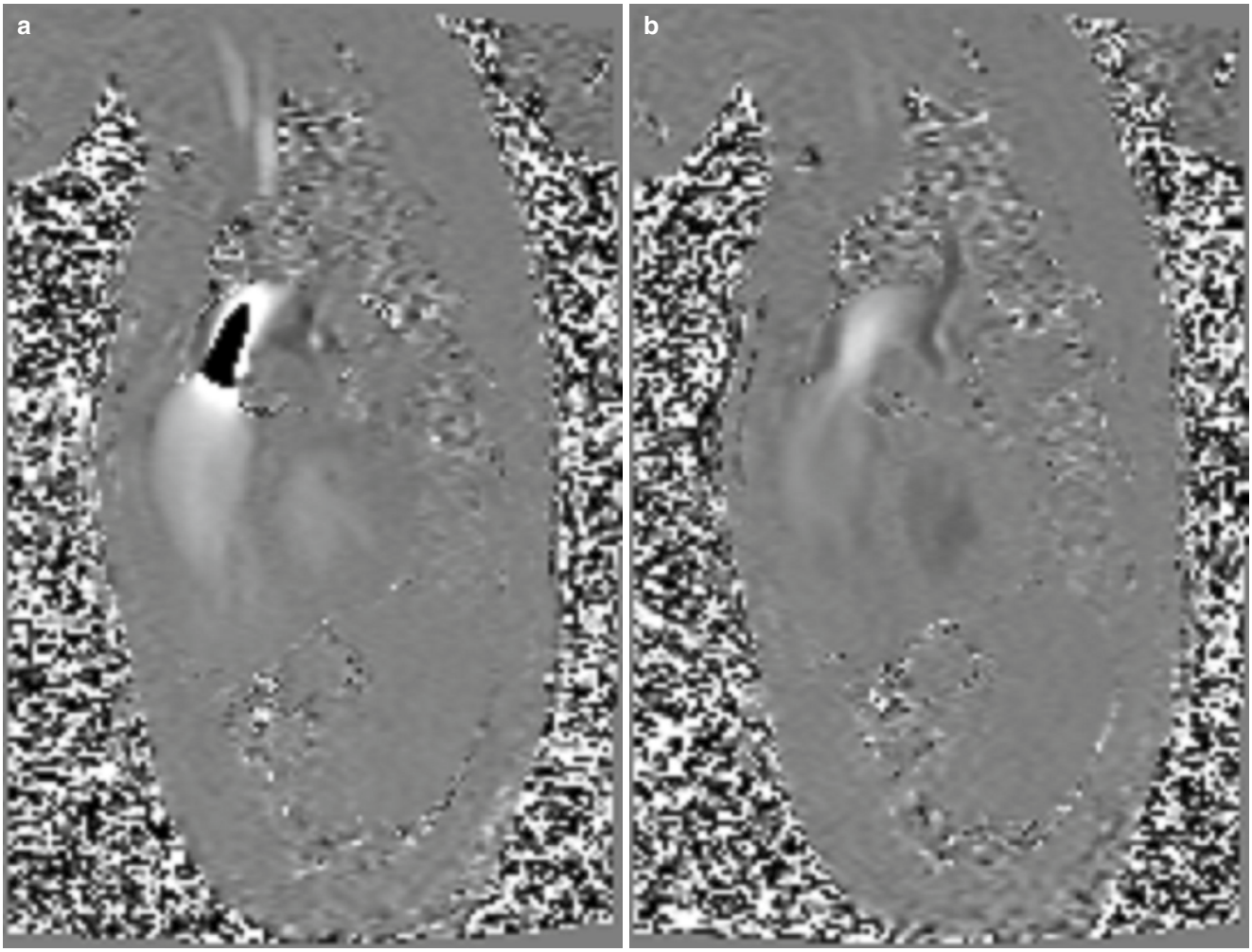

Fig. 16.5 Example of aliasing in the pulmonary artery. On the *left* the VENC value was set too low and the central jet of the flow appears dark, suggesting reverse flow (toward feet). The image on the right was taken with a higher VENC value and the aliasing disappears

Velocity Encoding Value (VENC)

The VENC value is a parameter set by the user and determines the time and magnitude of the applied bipolar velocity encoding gradients. The VENC essentially acts as a relation between the velocity values and the measured phase. If the measured phase exceeds +180°, or goes below −180°, it will be assigned a value within the 180° to +180° range since only 360° of phase can be measured. This condition is known as velocity aliasing or velocity wraparound, and an example from a patient is shown in Fig. 16.5. To avoid aliasing, a VENC value must be chosen so that aliasing does not occur. VENC values are displayed as the maximum velocity that can be measured without aliasing. This produces a difficulty in PCMR as the maximum velocity is not known a priori. When a good estimate of the maximum velocity cannot be made, a rapid scan can be done to check if aliasing is present. A VENC value that exceeds the maximum expected velocity but only by a small amount (~25 %) will maximize the ranges of phases used to measure velocity and hence increase the velocity-to-noise ratio. Additionally, it is important to realize that a smaller VENC value requires a larger gradient value, which will increase the echo time and may reduce the number of phases that can be acquired.

Specialized Implementations of PCMR

The majority of PCMR examinations are conducted using a single slice, 2D, ECG gated, cine implementation with velocity encoded through the slice plane to determine vessel flow as described above. However, several recent developments have enabled new applications that expand on this basic implementation and these are described below.

Alternate k-Space Sampling Strategies

Most work in PCMR has been done using standard Cartesian k-space sampling. One of the major problems using PCMR to quantify blood flow is the lengthy acquisition times associated with the technique. Multiple methodologies have been used to reduce acquisition time. Techniques such as vastly under-sampled radial projection reconstruction (VIPR) can be combined with PCMR [12]. PC-VIPR can reduce acquisition time of PC velocity images by sparsely sampling the edges of k-space and more densely sampling the central regions of k-space with a constrained radial sampling strategy. Interleaved spiral acquisition has also been used to reduce temporal resolution of the PCMR velocity measurements. The spiral technique has been used in a single slice, single direction mode to improve temporal resolution. These rapidly acquired images can be used to monitor short duration physiologic changes in cardiac output [13]. A third method to improve the acquisitions time is to use parallel imaging techniques with or without constrained reconstruction.

4D PCMR

The PCMR described previously can be expanded to measure multiple time-resolved velocity directions over a 3D volume (4D PCMR). As previously mentioned, creation of a PCMR image requires two underlying images (flow-encoded and flow compensated). Obtaining multiple directions of velocity increases this time, but advanced encoding strategies can limit the time to a maximum to four times that of the standard gradient echo sequence [14]. Implementing the technique with a 3D acquisition volume allows the voxel size to be reduced over a standard 2D acquisition, and allows for an integrated volume acquisition. Therefore, 4D PCMR can be used to completely define the three-dimensional, time-resoled velocity vector field over a 3D volume in vessels. Having this complete, time-resolved velocity field enables advanced visualization such as plotting streamlines, pathlines, and particle traces. A variety of cardiovascular applications have been examined with 4D PCMR, including ventricular flow and carotid flow, but applications in aortic disease has been a primary focus of many investigators [15, 16]. The major drawback to widespread use of 4D PCMR is the time required for acquisition. Even with parallel imaging techniques, acquiring velocity within the aorta requires ≈10 min.

Tissue Velocity Mapping

Similar to what has been done in ultrasound with tissue Doppler imaging (TDI), investigators have used PCMR to map velocity of the left ventricular myocardium rather than the blood flow [17]. This requires a low VENC value and a fairly high spatial resolution acquisition. The disadvantage is that these low VENC values requires a high velocity encoding gradient to generate adequate phase for the low velocities seen in the myocardial tissue (typically <10 cm/s). The higher gradient increases echo time, often causing susceptibility artifacts in the LV lateral wall, and reduces overall SNR within the image [17–20]. Other issues include the lengthy acquisition time required to cover the entire LV, and issues with large phase shifts from the flowing blood with in the left ventricle. Several applications, including measurement of ventricular dyssynchrony have shown promising results [20].

Real-Time PCMR

Because of the need for subtraction of two images in PCMR, development of real-time PCMR has lagged behind other MRI-based real time applications, such as cine imaging of the LV function, or monitoring of needles or catheters in interventional procedures. Using EPI or spiral acquisition and shared encoding strategies have allowed investigators to use real time PCMR to monitor exercise or stress-induced changes in aortic hemodynamics, and diagnosis of congenital and acquired pathology [21]. Because of the complex acquisition strategies and the required post-acquisition subtraction, there is often a delay in displaying the 'real-time' PCMR data. Investigators have employed and external dedicated reconstruction hardware to improve the time between delay and acquisition [22, 23].

Pulse Wave Velocity

Pulse wave velocity (PWV) can be used as a measure of arterial stiffness through the Moens-Korteweg equation. The PWV is most often estimated by dividing the distance between two measurement sites by the propagation time of the pressure or flow wave between the two sites. Two slices perpendicular to the aorta are most commonly used for recording locations, but multiple locations using in-plane flow encoding can also be used. A time-marker on the flow waveform must be chosen in order to compare pulse wave arrival times at the sites. High temporal resolution in the PCMR images is critical as the wavespeed is 3–10 m/s in the aorta [24, 25].

Post-processing of PCMR Data

Background Phase Correction

Despite the subtraction of velocity-encoded and non-encoded images, a background phase offset may remain in static tissue, causing static tissue to appear to have a small velocity. The phase offset is caused by concomitant gradients in phase-and by residual eddy currents. The phase offsets can be dependent on

position in the image, but generally are larger as the distance from the iso-center increases. Consideration of the background phase is important because a large background phase can affect the accuracy of flow measurements, especially when calculating quantities such as regurgitant fraction [26]. A variety of techniques have been employed to reduce the background phase or mitigate its effect on quantitative velocity measurements. From the acquisition side, it is important to keep the image slice and vessel near the iso-center of the magnet where effects of inhomogeneity and gradient eddy currents are minimal. From the post-processing side background phase effects can be removed with a background correction algorithm that can be automated, or use user-defined regions of interest place in static tissue.

Analysis of Velocity Images

By drawing a region of interest curve (ROI) around a vessel, statistics such as average velocity, peak velocity, and a velocity histogram can be determined in a region. One can multiply pixel area times the velocity value in each pixel to obtain flow for each frame. If the regions of interest (ROI's) are drawn for each time frame acquired, one can determine flow as a function of time over the cardiac cycle. Care is usually taken to trace boundaries near the edges of the vessel to eliminate contamination from other vessels, and to eliminate errors in the integration due to inclusion of excess static tissue.

Flow versus time curves can be used to determine clinically relevant quantities such as aortic regurgitant volume, abnormal ventricular filling patterns, cardiac stroke volume, cardiac output, quantification of volumetric flow in left-to-right shunts [27]. Advanced calculations can be done on the velocity maps to create parametric images of wall shear stress, pressure gradient, vorticity, etc.

Clinical Application of PCMR

A multitude of CMR techniques can aid in delineating specific etiologie and pathophysiology. CMR provides gold standard assessment of ventricular mass, volumes, wall motion, and viability via various cine and contrast enhancement techniques. PCMR provides a complementary hemodynamic assessment of systolic and diastolic function, further aiding both diagnosis and prognostication in patients with various cardiac diseases.

Myocardial Disease

Clinical heart failure may arise from impaired myocardial contraction, relaxation, or both conditions. Phase contrast magnetic resonance (PCMR) is useful in assessing the degree of both systolic and diastolic dysfunction due to various myocardial diseases, as well as impaired ventricular filling. The contribution of various myocardial, valve or shunt lesions to pressure and/or volume overload and secondary myocardial dysfunction can also be evaluated by PCMR.

Cardiac Output

Cardiac output (CO), is the product of stroke volume (SV) and heart rate and is an important clinical parameter in the assessment of patients with heart disease. Reduced CO or cardiac index (CI defined as CO/BSA) is the hallmark of systolic or diastolic dysfunction from any etiology. Traditionally, the most accurate method of measuring CO has relied on invasive cardiac catheterization. CMR offers a non-invasive measurement of CO by both cine ventricular volumetry and PCMR, both with accuracy and precision as comparable to invasive measures. Both CMR methods have established reference values, although cine ventricular volumetry is limited in the case of regurgitant valve disease.

The method of PCMR CO or SV measurement relies on a through-plane velocity measurement and integration of flow volume in one or both of the great vessels as described above. For LVSV measurement, the ascending aorta should be localized in an oblique sagittal scout image to visualize patient specific architecture. The PCMR imaging plane should be set perpendicular to the direction of flow. The location of the imaging plane relative to the aortic annulus is a matter of debate, as some groups recommend a proximal position between the annulus and sinotubular junction, while others recommend the mid-ascending aorta at the level of the main pulmonary artery (PA) bifurcation. The proximal position may be more susceptible to inaccuracies related to valve motion artifacts and complex flow patterns, however, it avoids error related to diastolic coronary flow. Measurement in the mid-ascending aorta, although felt to be more reproducible, may be more affected by aortic compliance, which underestimates regurgitant volume, and reverse coronary diastolic flow, which may account for 0.5–6 % of aortic forward flow. The VENC should initially be set at 200 cm/s.

RVSV is measured in main PA. The main PA should be localized in an oblique axial or coronal scout image to visualize the curvature. The imaging plane should be set perpendicular to the direction of flow, between the pulmonic valve and main PA bifurcation. The VENC should initially be = 200 cm/s. Comparison of the SV of the left and right ventricle (RV) may be used to provide an internal control, or to calculate Left-to-right's shunt ratio, if applicable.

Diastolic Dysfunction

Cardiac diastolic dysfunction is an abnormality of ventricular relaxation and occurs in a variety of heart failure etiologies. Diastolic heart failure is a predominant cause of heart failure

symptoms and may precede or accompany systolic dysfunction. Diastolic dysfunction is also a marker of poor outcomes, as patients with diastolic heart failure and preserved systolic function have similar mortality to patients with isolated systolic dysfunction [28, 29]. Diastology is also useful in the clinical management of patients, notably in the estimation of LV filling pressures and guidance of medical therapies.

Clinical diastolic function evaluation is most often performed with Doppler transthoracic echocardiography (TTE). Conventional parameters determined include early and late filling peak velocities of the transmitral flow (E and A waves), E-wave deceleration time (DT), and annular myocardial early longitudinal peak velocity (E′) and late longitudinal peak velocity (A′). Pulmonary vein peak systolic (S) and diastolic (D) velocities are a useful adjunct, specifically in the form of the S/D ratio.

CMR can offer a comprehensive evaluation of diastolic function comparable to Doppler TTE with the use of PCMR. PCMR derived diastolic hemodynamics will provide useful information in patients planned to undergo CMR or those with poor TTE windows. Additionally, PCMR may overcome certain limitations of Doppler TTE, including limited field of view, beam angle dependency, and incomplete sampling of eccentric flows.

Transmitral Flow Profiles

Cine CMR imaging in multiple long axis views should be used to visualize the mitral leaflets for planning a PCMR slice location to evaluate transmittal velocity. The PCMR slice should be prescribed at the leaflet tips during diastasis, parallel to the plane of the mitral annulus. Through-plane images should be acquired with retrospective EKG gating. An initial VENC setting around ~200 cm/s is reasonable. However, the correct VENC may vary, between 150 and >300 cm/s, depending on the patient's hemodynamics. After image acquisition, the ROI is traced around the inner contour of the mitral valve (MV) orifice in cross-section on magnitude images, and then transferred to phase images.

Transmitral peak E and A velocity waves are plotted on a flow versus time graph. The DT is calculated by subtracting the time of intersect of the peak E wave with the baseline from the time of intersect of the E wave downslope with the baseline. PCMR derived peak E and A velocity waves correlate well with Doppler TTE techniques, although there is a tendency towards underestimation of magnitude. Assessment of transmitral profiles and E/A ratio, however, have excellent agreement with Doppler TTE for identifying the presence and stage of diastolic dysfunction [30, 31].

Pulmonary Vein Flow Waveform

The right superior pulmonary vein is often the easiest to acquire on cine CMR or scout images, however, any or all visualized pulmonary vein may be imaged. The slice plane should be perpendicular to flow inside the vein, approximately 1 cm from the ostium. Through-plane PCMR images should be acquired with retrospective EKG gating and a VENC of 100 cm/s. After image acquisition, the ROI is traced around the inner lumen of the pulmonary vein on magnitude images, and then transferred to phase images. Pulmonary vein S and D average velocity waveforms are plotted on a velocity versus time graph to the time-dependent characteristics of the flow. PCMR derived pulmonary vein S/D ratio correlates well with Doppler TTE [32].

Mitral Annular Tissue Velocity

The basal lateral and/or basal septal segments of the mitral annulus can be visualized on long axis cine CMR imaging. A PCMR slice to measure mitral annular velocity should be placed at the lateral and/or septal MV annulus, with care to ensure it the slice does not include mid-left ventricular or left atrial myocardium. Through-plane PCMR images should be acquired with retrospective EKG gating and a VENC of 50 cm/s. After image acquisition, the ROI in the annulus is traced on magnitude images and transferred to phase images.

Mitral annular tissue average velocity waveforms are plotted on a velocity versus time graph to determine time-dependent velocity behavior of the tissue. PCMR derived mitral annular tissue velocities have been found to correlate well with tissue Doppler TTE [30, 33]. The E/E′ ratio has been found to correlate well between PCMR and Doppler TTE, as well. Importantly, PCMR derived E/E′ correlates strongly with invasive pulmonary capillary wedge pressure by cardiac catheterization with patients with E/E′ <8 have PCWP <15 mmHg and those with E/E′ >15 having PCWP >15 mmHg [20, 34].

Restrictive Physiology

Restrictive physiology may be a result of progressive diastolic dysfunction or restrictive cardiomyopathy. Restrictive cardiomyopathy often presents with signs of right heart failure including peripheral edema and ascites. Imaging findings include normal or reduced ventricular volumes and normal or near normal ventricular systolic function, often with significantly dilated atria. In this clinical setting, it is important to distinguish restrictive and constrictive physiology. Severe abnormalities of myocardial relaxation and filling, with E/A >2 and mitral annular tissue velocity <4 cm/s, is categorized as restrictive physiology. Moreover, CMR morphologic assessment and tissue characterization provides further analysis of specific causes of restrictive cardiomyopathy such as amyloidosis, sarcoidosis, hemochromatosis, Fabry's disease, endomyocardial fibrosis, and carcinoid heart disease [35].

Pitfalls

Diastolic transmitral hemodynamic profiles and mitral annular tissue velocities may be inaccurate due to large through-plane motion of the annulus over the cardiac cycle.

Specifically, transmitral diastolic velocities and flow may be underestimated. Visual confirmation and manual redrawing of the ROI at each cardiac phase to ensure the appropriate location over each cardiac cycle during post-processing may minimize error. Annular tracking with long-axis cine CMR navigators may provide motion compensation, although this technique is not widely available. The underestimation of peak E and A wave velocity magnitude with PCMR may be related to increased sensitivity of maximal velocity curves to noise or the temporal resolution of PCMR.

Pericardial Disease

CMR provides an accurate assessment of pericardial morphology including thickness, pericardial effusion, acute inflammation and fibrosis. CMR can also provide complementary functional and hemodynamic information on cine PCMR sequences.

Pericardial Constriction

Pericardial constriction occurs when normal ventricular diastolic filling is impeded by a non-compliant pericardium. In the clinical setting, it is critical to distinguish restrictive and constrictive physiology. Although pericardial thickening and even calcification may be present. This finding is not diagnostic of constriction, as constriction may exist without either finding [36, 37].

The hemodynamic hallmark of constriction is dissociation between intracardiac and intrathoracic pressures evidenced by ventricular interdependence and respiratory variations in atrioventricular valve inflow velocities, typically evaluated by Doppler TTE. CMR can provide an assessment similar to that of TTE, including volumetric and functional evaluation, identification of the interventricular septal bounce suggestive of ventricular interdependence and, inferior vena cava (IVC) plethora. Thorough hemodynamic evaluation is essential, as the interventricular septal bounce and IVC plethora may be seen in a variety of other conditions.

Pitfalls

Mitral and tricuspid annular motion with the cardiac cycle and respiration may displace the desired imaging plane on the horizontal long axis images, potentially introducing error into the flow measurements. This can be minimized by visual confirmation of enface inflow orientation with each frame during acquisition and redrawing of the ROI to ensure the appropriate location during post-processing.

Although the use of free-breathing acquisition improves temporal resolution, this may come at the expense of reduced signal-to-noise ratio. Furthermore, maximal velocity curves may have increased sensitivity to noise as they represent single time point in the cardiac cycle, compared to flow rates, which are estimated from the averaged velocity throughout the cycle. However, given the measurement of respiratory cycle-based velocity variation occurring over hundreds of milliseconds, this is unlikely to have significant impact.

Valve Disease

Left sided valve disease imposes a progressive hemodynamic burden on the heart in the form of pressure overload, volume overload, or both. Established criteria guide physicians in treating patients with left sided valve disease by incorporation of symptoms and cardiac structural changes, in addition to lesion severity as assessed by various imaging techniques. Quantitative assessment of lesion severity is preferred, and may facilitate intervention at an earlier stage prior to potentially irreversible structural changes and limiting symptoms. PCMR provides an accurate non-invasive estimate of hemodynamic profiles across any valve or vascular structure, and allows for precise quantitative results that may be complementary to the anatomic findings of both TTE and cine CMR. Transvalvular velocities, pressure gradients, flow rates, and flow volumes can be directly measured or calculated.

Aortic Stenosis

Aortic stenosis (AS) due to calcific degeneration is the most common valve disease of the elderly. However, congenital and rheumatic aortic valve (AV) disease may present as significant stenosis in children and young adults. Regardless of etiology, progressive narrowing of the AV orifice results in pressure overload of the LV with associated concentric remodeling and elevation of LV filling pressures. Surgical treatment decision is based on lesion severity and patient symptoms. AS is considered severe when the area of the valve orifice is less than 1 cm^2, the peak velocity is greater than 4 m/s, or the mean transvalvular gradient is more than 40 mmHg. PCMR imaging is useful in determining these structural and hemodynamic findings. Generally, the VENC should be based on the initially estimated severity and can be subsequently adjusted based on the presence of aliasing in the images. Cine CMR also provides complimentary structural assessment of valvular morphology, such as cusp number and fusion, and ventricular remodeling related to chronic pressure overload. Dynamic characterization of the valve orifice area, including morphology (i.e. bicuspid versus tricuspid) and direct measurement of the valve area is possible with PCMR. This method relies on visualization of a distinct boundary identifying high velocity pixels of the jet. The

imaging plane should be parallel to the AV annulus and use a short TE, high temporal resolution cine PCMR sequence.

Quantification of Peak Velocity and Transvalvular Pressure Gradients

The maximum instantaneous velocity (V_{max}) within the stenotic jet can be obtained on through-plane or in-plane PCMR. Through-plane analysis relies on slice positioning relative to the valve orifice, as the true V_{max} may be missed if the slice is too far from the valve orifice. Positioning too close to the valve orifice may result in inaccurate V_{max} from signal loss due to turbulent flow [38]. Conversely, in-plane analysis encompasses the entire longitudinal aspect of the jet, however, severe stenosis may result loss of accuracy due to partial volume averaging and movement of the jet out of the imaging plane. The use of both through-plane and in-plane imaging with sampling of the entire jet is recommended to maximize accuracy.

The peak transvalvular pressure gradient (ΔP) can be calculated using the modified Bernoulli equation and V_{max} as:

$$\Delta P = 4\left(V_{max}\right)^2$$

Measurement of velocities and pressure gradients by PCMR correspond well with both Doppler TTE and cardiac catheterization.

Pitfalls

Partial volume averaging results from increased voxel size due to large slice thickness and causes averaging of velocities from inside and outside of the vena contracta. The net effect of partial volume may be underestimation of the true peak velocity, which has been reported in multiple studies comparing PCMR to Doppler TTE. Generally, thin-section imaging with overlapping and a minimum of 16 voxels covering a cross section volume is adequate to avoid significant partial volume effects [39]. Alignment of the flow jet and imaging plane may be challenging with eccentric high velocity jets and horizontally oriented aortic annuli. Errors related to flow-plane misalignment is proportional to the cos θ, where θ is the angle of misalignment, thus a small degree of misalignment is associated with a small error. Stenotic AVs are often heavily calcified, which may subject images to significant susceptibility artifact, limiting hemodynamic evaluation at the level of the valve plane.

Aortic Regurgitation

Aortic regurgitation (AR) may arise from primary abnormalities of the aortic valve leaflet or secondary to aortic root dilatation. The primary hemodynamic consequence of chronic AR is progressive LV volume overload which may remain asymptomatic for years. The timing of surgery for severe AR depends on the presence of symptoms or significant chamber dilatation in asymptomatic patients. Grading of AR has traditionally relied on qualitative and semi-quantitative findings on Doppler TTE or aortic root angiography. Quantitative parameters such as regurgitant jet area, regurgitant volume (RVol), and regurgitant fraction (RF; RVol divided by total LV SV) are the strongest indicators of true lesion severity. A variety of PCMR derived CMR approaches are useful for AR quantification and provide a non-invasive, alternative to traditional methods. AR grading by CMR derived RF is generally accepted as: mild, RF less than 15 %; moderate, RF 16–25 %; moderate to severe 25–48 % and severe, greater than 48 % [40]. Retrospective ECG gating should be utilized to ensure the entirety of diastole is appraised. Cine CMR is used to provide clues as to AR etiology such as jet location and direction, leaflet prolapse or perforation, annular morphology and aortic abnormalities such as root dilatation or aortic dissection. Assessment of LV chamber dimensions is a vital complement to PCMR hemodynamic data.

Calculation of Regurgitant Fraction from Transaortic and Transpulmonic Flows

Direct through-plane measurement of blood flow in the ascending aorta and main PA will provide an assessment of left and right ventricular SVs, respectively, when integrated throughout systole. In the absence of intracardiac shunting or valvular regurgitation, the difference between right and LV volumes by CMR is less than 5 %. This method allows calculation of the RF as:

$$RF = \left[\left(LVSV - RVSV\right)/LVSV\right]*100$$

The assessment of LVSV and RVSV by PCMR correlate well with Doppler TTE and invasive cardiac catheterization derived measures [41]. This method assumes isolated AR and is invalid in the case of multivalvular regurgitation.

Quantification of Regurgitant Fraction from Transaortic Flow

An accurate and reproducible method of AR quantification by PCMR is direct through-plane measurement of antegrade and retrograde proximal aortic flow throughout the cardiac cycle. Aortic flow is plotted versus time, and the area inside the curve under the baseline represents diastolic retrograde flow. Systolic antegrade flow, that is LVSV. The Regurgitant Fraction (RF) is calculated as:

$$RF = \left(RVol/LVSV\right)*100$$

It is important to place the slice plane perpendicular to the direction of flow in the aortic root. The plane should be

placed proximal to the coronary ostia, as close to the valve as possible, without artifacts from valve motion and complex flow patterns. This position may also demonstrate the site of regurgitation. Multiple scout views are helpful to account for obliquity and proper placement. This method correlates well with the CMR method of biventricular volumetry, as well as Doppler TTE and aortic root angiography [42].

The presence of valve motion artifacts and complex flow patterns in the proximal root has led some to recommend aortic flow measurement in the mid-ascending aorta at the site of the right PA. However, this position may be more affected by aortic compliance, which underestimates RVol, and reverse coronary diastolic flow, which may account for over 6 % of aortic forward flow [43].

Mitral Stenosis

Mitral stenosis (MS) is caused by restriction of MV opening involving any portion of the mitral apparatus and the result is LV inlet obstruction with a diastolic transvalvular pressure gradient between the left atrium and LV. MS is considered severe when the area of the valve orifice is less than 1 cm^2 and/or the mean transvalvular gradient is more than 10 mmHg. PCMR provides quantitative hemodynamic information complemented by leaflet, chordae, and annular morphology, planimetered valve area, and abnormal chamber size, such as left atrial enlargement and small LV, seen on cine CMR.

Quantification of Peak Velocity and Transvalvular Pressure Gradient

The calculation of V_{max} should be performed in multiple in-plane and through-plane positions perpendicular and parallel to the direction of flow. As in AS, through-plane analysis relies on slice positioning relative to the valve orifice, as the true V_{max} may be missed if the slice is too far from the valve orifice. Positioning too close to the valve orifice may result in inaccurate V_{max} from signal loss due to turbulent flow. Conversely, in-plane analysis encompasses the entire longitudinal aspect of the jet, but in the setting of severe stenosis may result in loss of accuracy due to partial volume averaging and movement of the jet out of the imaging plane. The use of thin-section imaging may resolve this problem. The use of both through-plane and in-plane imaging with sampling of the entire jet is recommended to maximize accuracy. An initial VENC setting around 200 cm/s is reasonable. However, the correct VENC may vary, between 150 and 400 cm/s, depending on the patient's hemodynamics. The peak transvalvular pressure gradient (ΔP) can be calculated using the modified Bernoulli equation and V_{max} as:

$$\Delta P = 4\left(V_{max}\right)^2$$

The mean transvalvular pressure gradient is obtained by averaging all of the instantaneous velocities over systole. Generally, the mean pressure gradient is about two-third of the peak pressure gradient. Measurements of velocities and pressure gradients by PCMR correspond well with Doppler TTE [44].

Pitfalls

Atrial fibrillation, which is common in MS patients, limits the utility of PCMR quantification due to significant variation in cardiac cycle length. Partial volume effects may result in underestimation of peak velocity and pressure gradients; increased flow states may cause increased peak velocity and pressure gradients similar to AS. Stenotic MVs are often heavily calcified, which may subject images to significant susceptibility artifact, limiting hemodynamic evaluation at the level of the valve plane.

Mitral Regurgitation

Mitral regurgitation (MR) may occur due a primary valve abnormality, such as leaflet prolapse or perforation, or chordal rupture causing a flail leaflet. The etiologies of these abnormalities include, but are not limited to, age related degeneration, myxomatous infiltration, and endocarditis. Alternatively, MR may be secondary to ventricular abnormalities such as papillary muscle dysfunction in ischemic heart disease, or a dilated mitral annulus with dilated cardiomyopathy. A consequence of primary MR is increased LVSV. Surgical intervention for severe MR is predicated by symptoms and structural remodeling, including drop in EF below 60 % and increase in LV end-systolic dimension greater than 4 mm in asymptomatic patients [45]. Currently, Doppler TTE is most commonly used for diagnosis and in the case of poor TTE windows or discrepant results, quantitative parameters such as Regurgitant volume (R_{Vol}) and RF can be obtained by a variety of PCMR derived CMR approaches. MR grading by CMR derived RF is generally accepted as: mild, RF less than 15 %; moderate, RF 16–25 %; moderate to severe 26–48 % and severe, greater than 48 % [40]. Cine CMR provides a complimentary assessment of leaflet, subvalvular, and annular morphology, as well as a gold standard of chamber and volume quantification.

Calculation of Regurgitant Fraction from Cine Volumes and Great Vessel Flows

The most dependable method of MR quantification utilizes a combination of through-plane transaortic, and LVSV measured on cine CMR. The LVSV is the difference of the LV end-diastolic volume and LV end-systolic volume. The difference between the LVSV and aortic valve SV represents the R_{Vol}. The Regurgitant Fraction (RF) is calculated as:

$$RF = \left[\left(LVSV - \text{semilunar valve SV}\right) / LVSV\right] * 100$$

This method correlates well with both Doppler TTE and cardiac catheterization [42, 46]. In the case of significant AR, the transpulmonic SV can be used, providing there is no significant Pulmonary Regurgitation.

Pitfalls

Direct diastolic transmitral flow measurement may be difficult due to valve motion with the cardiac cycle and the three-dimensional "saddle shape" of the mitral annulus. Annular tracking with long-axis cine CMR images may provide motion compensation, although not widely available. A control volume approach can overcome many of these issues, but is time consuming [47].

Prosthetic Valves

Both surgical and percutaneous prosthetic valves can be safely imaged by CMR. Poor visualization due to susceptibility artifact may limit morphologic assessment and measurement of transvalvular velocity and pressure gradients by PCMR, however, downstream hemodynamic assessment remains possible [48, 49]. PCMR is particularly helpful in the assessment of prosthetic valve dysfunction or paravalvular pathology associated with significant regurgitation, as TTE is often limited by significant attenuation from metal containing prostheses.

Methods utilizing cine CMR volumetric analysis and through-plane aortic flow assessment are valid, with additional considerations. Surgical aortic valves generally have a low profile in the aortic root, allowing through-plane flow analysis in proximity to the valve. Transcatheter valves generally have a higher profile within the aorta due to the valve stent frame, with the Edwards Sapien valve extending nearly 1 cm into the aortic root and the Medronic CoreValve extending 2–3 cm into the aortic root. The nitinol stent frame of the Medtronic CoreValve produces little susceptibility artifact allowing flow analysis in the aortic root.

Vascular Disease

Diseases of the aorta and peripheral vessels are commonly imaged with MRA techniques, however, PCMR provides useful functional information complementary to MRA morphology findings. In the setting of Aortic Dissection, in-plane and through plane views are both useful in distinguishing the true and false lumens. High-velocity flow will be seen in the true lumen, while lower velocities will be seen in the false lumen, often with bidirectional flow. Retrospective gating should be utilized, with an initial VENC of 150 cm/s. Pressure gradients due to Aortic coarctation or atherosclerotic lesions can be estimated with the modified Bernoulli equation [50].

Congenital Heart Disease

One of the areas where PCMR has been used most extensively is congenital abnormalities. The complex anatomy and often widely varying hemodynamics make PCMR particularly useful. Here we describe how PCMR is used in some of the most common pediatric applications.

Coarctation of the Aorta

Initially thought to be a simple lesion involving narrowing of the aorta at the junction of the distal aortic arch and descending thoracic aorta, coarctation has been recognized to be a complex disorder which requires life-long follow-up and serial imaging even after surgical or interventional treatment [51]. The underlying cause of coarctation it not known though it is believed to be related to postnatal constriction of aberrant ductal tissue.

When using CMR to evaluate the patient with untreated repaired coarctation, it is important to note the nature of the lesion (local stenosis or longer segment stenosis), presence of other associated defects (predominantly bicuspid aortic valve or aortic aneurysm). In the surgically or percutaneously palliated patient, the key to assessment involves an understanding of the type of repair. Resection and end to end anastomosis is the most common type of repair; particularly in the young child. Other types of repair are less common but occasionally are required depending on surgical considerations.

PCMR can provide a hemodynamic assessment of lesion severity and define the presence or absence of collateral blood flow. Due to signal void artifact present in patients who undergo percutaneous stent repair of this lesion, CMR can be limited in the assessment of these patients.

In patients with native coarctation, defining the anatomy of the lesion is the most important portion of the procedure. Unless the imaging planes are properly prescribed, hemodynamic assessment by PCMR will be difficult. MR angiography provides the simplest and most effective way to identify pertinent anatomy. MRA protocol uses 0.1–0.2 mmol/kg of gadolinium contrast injected at 2–3 ml/s using bolus detection with initial acquisition starting once contrast is visualized in the left ventricle. Two repeat acquisitions are then obtained immediately following the initial acquisition. Anatomic planes for hemodynamic evaluation can then be prescribed using the 3-D tool on the work-station. For patients that have contra-indication to gadolinium contrast

other non-contrast techniques are available to provide anatomic data, most notably the use of dark-blood imaging obtained in an axial plane. Prescribing an imaging plane across the ascending aorta through the descending aorta will result in an oblique sagittal view of the thoracic aorta and coarctation segment. This typically prescribes an imaging plane that is inclusive of the ascending aorta, arch, and descending aorta including the coarctation segment.

The most critical aspect of the hemodynamic assessment of the unrepaired coarctation is an assessment of the pressure gradient across the lesion. Traditionally a gradient >20 mmHg is considered to be significant, and this gradient was measured using the difference in systolic blood pressure between the right arm and left leg. This clinical exam is often unreliable in assessment of the true pressure difference particularly in patients with extensive collateral formation. PCMR is an accurate and reproducible method of assessing this gradient. This gradient is best obtained by first obtaining an in-plane flow in the descending thoracic aorta and identifying the segment where maximum velocity occurs. A through plane velocity can then be obtained at this level thereby obtaining a true peak velocity. Using the modified Bernoulli equation, the peak gradient can then be obtained.

Another unique feature of PCMR imaging is the assessment of collateral flow in coarctation. This is usually achieved by a comparison of the measurement of flow in the proximal descending thoracic aorta to the descending thoracic aorta just above the level of the diaphragm. Collateral flow can be assumed to be present if the flow in the descending thoracic aorta just above the diaphragm is greater than the flow in the proximal descending thoracic aorta. This occurs because the intercostal arteries become engorged with blood and other collateral vessels form causing blood flow down the internal mammary arteries and retrograde from the intercostal arteries increasing the flow in the descending thoracic aorta. This creates the characteristic rib notching seen on chest x-ray. The percent increase in flow in the descending thoracic aorta is directly related to the degree of stenosis. Thus, it serves as an indicator of the degree of hemodynamic compromise.

Intracardiac Shunts

Intracardiac shunts are a hallmark of congenital heart disease. In the pediatric realm, atrial septal defects (ASD) represent 1 in 1,500 live births. Most adults who present to a physician with an undiagnosed congenital heart disease do so with an ASD. The management of these defects is dependent on two items measured in tandem – the anatomy of the defect and the physiologic repercussions. CMR is well-suited for the evaluation of ASD shunt anatomy and physiology. Ventricular septal defects (VSD) are the most common congenital heart lesion and can also be visualized by CMR. Small, isolated ventricular septal defects often close in the pediatric years without intervention and are not present in adulthood. In the developed world, patients with larger VSDs are typically identified early and undergo corrective or palliative surgery.

In-plane PCMR imaging can allow for identification of the defect and visualization of left to right or right to left shunting. Compared with measurements obtained during cardiac catheterization, thru plane PCMR of flow in the proximal great vessels can reliably assess the magnitude of intracardiac left-to-right shunting [52].

Atrial Septal Defects

Secundum atrial septal defects represent the most common type of atrial level defect. They are slightly more common in females and result from defective growth of the septum secundum or excessive resorption of the septum primum. This defect, even in late adulthood, is predominantly left to right in shunt flow as the pulmonary bed has a high capacitance. The presence of right to left shunting is fairly rare even with large defects, but when present suggests pulmonary arterial hypertension.

PCMR can be used to quantify the shunt fraction in patients with this defect by calculating the ratio of pulmonary to aortic flow.

$$\mathrm{Qp}/\mathrm{Qs} = \left(\text{Pulmonary forward flow} / \text{Aortic forward flow}\right)$$

While Qp/Qs is typically a reliable measure for shunt flow there can be some pitfalls. Most notable is significant pulmonic or aortic regurgitation as this negative flow in proximal great vessels would increase the forward flow of the next cardiac cycle increasing the cardiac output and thus altering the Qp/Qs calculation. The size of the shunt could be incorrectly increased or decreased. Theoretically, small defects would gain unnecessary importance in the presence of significant pulmonary regurgitation, and larger shunts would appear diminished in the presence of significant aortic regurgitation. Another concern is when the shunt ratio is low (below 1.3) as there is no clear threshold delineating shunt presence from absence by PCMR. Hence while Qp/Qs analysis is important in understanding the hemodynamic implications of the shunt; it should not be used in isolation. A thorough interrogation of the atrial septum is required to rule out small secundum defects that appear insignificant by Qp/Qs calculation.

Sinus venosus ASDs occur in two forms – inferior and superior. Superior sinus venosus defects are the more common of the two and arise at SVC/RA junction superior to the fossa ovalis. Additionally, there is a significant association of partial anomalous return of the right superior pulmonary vein into the superior vena cava. This leads to an increase in

the degree of left to right shunting as compared to secundum defects. PCMR can be used to quantify the degree of shunting as described for secundum defects above. PCMR, specifically in-plane velocity mapping, can also be used to identify anomalous pulmonary vein flow. This is particularly important as PCMR can reliably detect and quantify these lesions even when other imaging modalities have not readily identified the defect. Inferior sinus venosus defects are much less common and are located at the junction of the right atrium and IVC and is associated with anomalous right inferior pulmonary vein.

Ventricular Septal Defects

While large atrial septal defects rarely lead to pulmonary arterial hypertension (PAH) in the adult, an uncorrected VSD will lead to PAH and subsequent right to left shunting manifesting as a Qp/Qs to <1.

Rarely, adults may present with new symptoms of exercise intolerance as a result of a moderate VSD associated with a left-to-right shunting leading to LV dilation. Unlike ASD which result in right heart enlargement, moderate to large sized VSD will cause left sided ventricular enlargement as the LV receives the excess shunted blood back from the pulmonary circuit. In these cases, where significant pulmonary arterial hypertension has not occurred the shunt fraction will remain >1.5.

Most VSDs identified in adulthood are small restrictive defects that do not alter cardiac hemodynamics. In these cases, shunt fraction by PCMR is undetectable or negligibly increased and RV/LV stroke volumes are similar assuming the absence significant valvular heart disease.

Pulmonary Valve Disorders

Pulmonary valve disorders are typically due to congenital heart disease. Congenital pulmonary stenosis treated in the infant can result in either regurgitation or stenosis. Pulmonary valve assessment is critical in patients with Tetralogy of Fallot (TOF). TOF is the most common cyanotic heart defect and is also one of the most common indications for a congenital CMR exam. The treatment of these patients has changed dramatically with advances in surgical and medical therapy. The original repair involved closure of the ventricular septal defect and resection of muscle from the infundibular region of the right ventricular (RV) outflow tract. In many cases this still resulted in a fair degree of RV outflow obstruction due to reduced pulmonary annulus size. Surgeons compensated for this by using a transannular patch. This relieved the RV outflow tract obstruction but resulted in varying degrees of pulmonic regurgitation, often severe. While severe pulmonic regurgitation can be tolerated well for years to decades it can lead to deleterious effects on the RV and also lead to potentially fatal arrhythmias. Thus, the question of when to replace the pulmonary valve and how to classify the degree of pulmonic regurgitation is of significant importance in the patient with repaired TOF. Though echocardiography plays a valuable role in this assessment, CMR outperforms echo in this assessment [53]. CMR and PCMR are ideally suited for the evaluation of the pulmonary valve.

Regurgitant fraction (RF) as described previously is defined as the regurgitant flow (ml/beat) divided by the forward flow (ml/beat) and is typically expressed by percentage:

$$RF = \left(\text{Re}\,gurgi\,\tan t\,Flow / Forward\,Flow\right)\times 100 = \left[\left(RVSV - LVSV\right) / RVSV\right]$$

In pulmonary valve disorders mild regurgitation is classified as <20 %, moderate is 20–40 %, and severe is >40 %. Some consider 30–40 % to represent a subset of patients with moderate to severe regurgitation [53]. Patients with moderate to severe or severe pulmonary regurgitation that are those typically considered for pulmonary valve replacement when appropriate indications are met. CMR criteria for pulmonary valve replacement in *asymptomatic* patients with severe PR include development of at least two of the following criteria [54]:

(a) RV/LV volume ratio greater than 2:1
(b) RVEDV index >150 mL/m^2
(c) Large akinetic areas seen along RVOT
(d) RV ejection fraction <47 %
(e) RV end-systolic volume index >80 ml/m2
(f) Left-to-right shunt from residual atrial or ventricular septal defects with pulmonary-to-systemic flow ratio ≥1.5
(g) Severe aortic regurgitation, RF > 48 %

For accurate assessment of pulmonary valve flow the imaging plane should be perpendicular to the RVOT at a level just above the pulmonary valve. In order to obtain a true perpendicular imaging plane planning should be done using two separate oblique RVOT views.

In-plane velocity encoding imaging can also be obtained in the RVOT views to help visually assess the degree of regurgitation; though it is not as accurate as through plane estimation which allows for true quantification. A high-velocity jet visualized by in-plane velocity mapping can be useful for locating the appropriate through-plane acquisition. This is particularly important when evaluating pulmonary stenosis. Through-plane flow quantification is significantly more reliable when the imaging plane transects the point of maximum velocity which is typically just downstream from the orifice of the lesion in question. The jet core can be recognized as the area of aliasing on velocity maps (black over white or white over black flow).

The peak pressure gradient across a stenotic lesion can be measured by knowing the maximum peak systolic velocity (V_{max}) and using the modified Bernoulli equation.

$$\text{Pressure gradient}\left(\text{mmHg}\right) = 4 \times \left(V_{max}\right)^2$$

The grading of pulmonic stenosis is typically defined by either the peak velocity or peak gradient:

Degree of stenosis	Peak velocity (m/s)	Peak gradient (mmHg)
Mild	<3	<36
Moderate	3–4	36–64
Severe	>4	>64

Progression of pulmonary stenosis is rare and patients with a peak gradient below 50 mmHg typically do not progress to severe pulmonic stenosis. When pulmonary stenosis is suspected CMR imaging can provided added value. It is useful in the determining the level of obstruction e.g.: infundibular, valvular, or subvalvular as well as help define any associated lesions such as pulmonary artery stenosis, intracardiac shunts, or coexisting pulmonary regurgitation. Asymptomatic patients with valvular PS with gradients of greater than 60 mmHg should have relief of the obstruction, most commonly by percutaneous balloon valvuloplasty.

Pulmonary Hypertension

Pulmonary hypertension is defined as an elevated mean pulmonary arterial pressure greater than 25 mmHg at rest. Pulmonary hypertension is often related to elevated left sided pressures, leading to the diagnosis of pulmonary venous hypertension. Pulmonary arterial hypertension is diagnosed when the mean pulmonary arterial pressure is greater than 25 at rest and the left ventricular end diastole pressure or the mean pulmonary capillary wedge pressure is less than 15 mmHg. The initial work-up typically involves a thorough history/physical, echocardiography, and right heart catheterization. Further diagnostic imaging is then based upon the results of this evaluation.

While echocardiography plays the primary role as the screening tool for patients with PAH, CMR is ideally suited for assessment of the right ventricle and the proximal pulmonary arteries. Hence there has been great interest in the development of CMR and velocity flow mapping in the diagnosis and hemodynamic evaluation of pulmonary arterial hypertension. While it is difficult to use CMR alone to establish a cause for PAH, there are patients who can benefit from information provided by CMR. Patients in research trials or on therapy with PAH drugs may particularly benefit with CMR for serial re-evaluation of RV function and size. The use of PCMR has also been studied in the PAH population and has both its benefits and drawbacks [55, 56].

PCMR, particularly of the tricuspid valve, is limited in the evaluation of PAH. Unlike echocardiography where tricuspid continuous wave Doppler accurately identifies the right ventricular systolic pressure, it is not possible to do so with PCMR. This is a result of fairly rapid dispersion of multiple small jets cores that are too small to be measured either by in plane or through plane flow mapping. PCMR of the pulmonary artery can be used to track cardiac output; additionally PCMR derived flow in the main pulmonary artery has also been used to indirectly assess the hemodynamics of pulmonary hypertension. Pulmonary arterial pressures are inversely correlated with average blood velocity in the main PA. It also appears to have consistent performance across different subgroups of PAH.

PCMR also demonstrates an inhomogeneous flow profile in the pulmonary artery in patients with pulmonary hypertension. Compared to healthy controls, patients with PAH have lower peak systolic velocity and greater retrograde flow after middle to late systole. Retrograde flow observed in patients with PH is also a hemodynamic indication of severity. It is inversely proportional to pulmonary flow volume and directly proportional to pulmonary resistance and cross-sectional area of the vessel. Additionally, 3D magnetic resonance phase-contrast imaging of the main pulmonary is a novel tool in the assessment of PAH. Mean pulmonary pressures by 4D PCMRI have been shown to be within 3–4 mmHg of cardiac catheterization derived values [57].

Other metrics have also been studied in CMR for the assessment of pulmonary arterial hypertension. Pulmonary artery strain, acceleration volume, pressure wave velocity, amongst others has been studied with varying degrees of success [58]. The significant number of non-invasive measures many of which require a fair amount of time in calculation and post-processing makes their clinical usefulness limited. The average velocity of main pulmonary artery flow is currently the most clinically useful tool in the hemodynamic evaluation of PAH as it fairly technically easy to obtain without the need for significant post-processing. Advantages in using an average PA velocity include the lack of assumption of a uniform PA profile which is known to be fairly inhomogeneous in PAH. However, this PA profile is typically obtained by PCMR with breath-hold sequencing which can take in the range of 15–20 s. This can be challenging in patients with pulmonary arterial hypertension particularly if they require supplemental oxygen at baseline. Current real-time non-breathhold flow imaging has not been thoroughly evaluated in this population and thus CMR derived measures are not yet capable of completely replacing right-heart catheterization in the evaluation of PAH.

Conclusion

CMR is routinely used in a variety of cardiovascular abnormalities to quantitatively measure blood velocity and

determine flow. The most widely used technique to quantify blood flow is *Phase-Contrast Magnetic Resonance* (*PCMR*), also called phase velocity mapping, phase velocity encoding, quantitative flow imaging, etc. The implementation of PCMR in clinical practice requires understanding of physical principles of image generation, pulse sequences, acquisition methods and analysis. Clinical applications include valvular heart disease, congenital heart disease, vascular disease and myocardial disease.

References

1. Morse OC, Singer JR. Blood velocity measurements in intact subjects. Science. 1970;170(3956):440–1. PubMed PMID: 5460060.
2. Rittgers SE, Fei DY, Kraft KA, Fatouros PP, Kishore PR. Velocity profiles in stenosed tube models using magnetic resonance imaging. J Biomech Eng. 1988;110(3):180–4. PubMed.
3. Oshinski JN, Ku DN, Pettigrew RI. Turbulent fluctuation velocity: the most significant determinant of signal loss in stenotic vessels. Magn Reson Med: Off J Soc Magn Reson Med Soc Magn Reson Med. 1995;33(2):193–9. PubMed.
4. Guilfoyle DN, Gibbs P, Ordidge RJ, Mansfield P. Real-time flow measurements using echo-planar imaging. Magn Reson Med: Off J Soc Magn Reson Med Soc Magn Reson Med. 1991;18(1):1–8. PubMed.
5. Keegan J, Gatehouse PD, Yang GZ, Firmin DN. Spiral phase velocity mapping of left and right coronary artery blood flow: correction for through-plane motion using selective fat-only excitation. J Magn Reson Imaging. 2004;20(6):953–60. doi:10.1002/jmri.20208. PubMed PMID: 15558551.
6. Markl M, Alley MT, Pelc NJ. Balanced phase-contrast steady-state free precession (PC-SSFP): a novel technique for velocity encoding by gradient inversion. Magn Reson Med: off J Soc Magn Reson Med Soc Magn Reson Med. 2003;49(5):945–52. doi:10.1002/mrm.10451. PubMed.
7. Spraggins TA. Wireless retrospective gating: application to cine cardiac imaging. Magn Reson Imaging. 1990;8(6):675–81. PubMed.
8. Tang C, Blatter DD, Parker DL. Correction of partial-volume effects in phase-contrast flow measurements. J Magn Reson Imaging. 1995;5(2):175–80. PubMed.
9. Oshinski JN, Ku DN, Mukundan Jr S, Loth F, Pettigrew RI. Determination of wall shear stress in the aorta with the use of MR phase velocity mapping. J Magn Reson Imaging. 1995;5(6):640–7. PubMed.
10. Markl M, Chan FP, Alley MT, Wedding KL, Draney MT, Elkins CJ, Parker DW, Wicker R, Taylor CA, Herfkens RJ, Pelc NJ. Time-resolved three-dimensional phase-contrast MRI. J Magn Reson Imaging. 2003;17(4):499–506. doi:10.1002/jmri.10272. PubMed.
11. Johnson K, Sharma P, Oshinski J. Coronary artery flow measurement using navigator echo gated phase contrast magnetic resonance velocity mapping at 3.0 T. J Biomech. 2008;41(3):595–602. doi:10.1016/j.jbiomech.2007.10.010. PubMed PMID: 18036532, PubMed Central PMCID: PMC2759278.
12. Gu T, Korosec FR, Block WF, Fain SB, Turk Q, Lum D, Zhou Y, Grist TM, Haughton V, Mistretta CA. PC VIPR: a high-speed 3D phase-contrast method for flow quantification and high-resolution angiography. AJNR Am J Neuroradiol. 2005;26(4):743–9. PubMed.
13. Carvalho JL, Nayak KS. Rapid quantitation of cardiovascular flow using slice-selective fourier velocity encoding with spiral readouts. Magn Reson Med: Off J Soc Magn Reson Med Soc Magn Reson Med. 2007;57(4):639–46. doi:10.1002/mrm.21196. PubMed.
14. Dumoulin CL, Souza SP, Darrow RD, Pelc NJ, Adams WJ, Ash SA. Simultaneous acquisition of phase-contrast angiograms and stationary-tissue images with Hadamard encoding of flow-induced phase shifts. J Magn Reson Imaging. 1991;1(4):399–404. PubMed.
15. Hope MD, Sedlic T, Dyverfeldt P. Cardiothoracic magnetic resonance flow imaging. J Thorac Imaging. 2013;28(4):217–30. doi:10.1097/RTI.0b013e31829192a1. PubMed.
16. Markl M, Schnell S, Barker AJ. 4D flow imaging: current status to future clinical applications. Curr Cardiol Rep. 2014;16(5):481. doi:10.1007/s11886-014-0481-8. PubMed.
17. Van Dijk P. Direct cardiac NMR imaging of heart wall and blood flow velocity. J Comput Assist Tomogr. 1984;8(3):429–36. PubMed.
18. Delfino JG, Bhasin M, Cole R, Eisner RL, Merlino J, Leon AR, Oshinski JN. Comparison of myocardial velocities obtained with magnetic resonance phase velocity mapping and tissue Doppler imaging in normal subjects and patients with left ventricular dyssynchrony. J Magn Reson Imaging. 2006;24(2):304–11. doi:10.1002/jmri.20641. PubMed.
19. Delfino JG, Johnson KR, Eisner RL, Eder S, Leon AR, Oshinski JN. Three-directional myocardial phase-contrast tissue velocity MR imaging with navigator-echo gating: in vivo and in vitro study. Radiology. 2008;246(3):917–25. doi:10.1148/radiol.2463062155. PubMed.
20. Marsan NA, Westenberg JJ, Tops LF, Ypenburg C, Holman ER, Reiber JH, De Roos A, Van der Wall EE, Schalij MJ, Roelandt JR, Bax JJ. Comparison between tissue Doppler imaging and velocity-encoded magnetic resonance imaging for measurement of myocardial velocities, assessment of left ventricular dyssynchrony, and estimation of left ventricular filling pressures in patients with ischemic cardiomyopathy. Am J Cardiol. 2008;102(10):1366–72. doi:10.1016/j.amjcard.2008.06.064. PubMed.
21. Korperich H, Gieseke J, Barth P, Hoogeveen R, Esdorn H, Peterschroder A, Meyer H, Beerbaum P. Flow volume and shunt quantification in pediatric congenital heart disease by rea KOWALIK GT l-time magnetic resonance velocity mapping: a validation study. Circulation. 2004;109(16):1987–93. doi:10.1161/01.CIR.0000126494.66859.A2. PubMed.
22. Kowalik GT, Steeden JA, Pandya B, Odille F, Atkinson D, Taylor A, Muthurangu V. Real-time flow with fast GPU reconstruction for continuous assessment of cardiac output. J Magn Reson Imaging. 2012;36(6):1477–82. doi:10.1002/jmri.23736. PubMed.
23. Lin HY, Bender JA, Ding Y, Chung YC, Hinton AM, Pennell ML, Whitehead KK, Raman SV, Simonetti OP. Shared velocity encoding: a method to improve the temporal resolution of phase-contrast velocity measurements. Magn Reson Med: Off J Soc Magn Reson Med Soc Magn Reson Med. 2012;68(3):703–10. doi:10.1002/mrm.23273. PubMed PMID: 22139889, PubMed Central PMCID: PMC3339280.
24. Suever JD, Oshinski J, Rojas-Campos E, Huneycutt D, Cardarelli F, Stillman AE, Raggi P. Reproducibility of pulse wave velocity measurements with phase contrast magnetic resonance and applanation tonometry. Int J Cardiovasc Imaging. 2012;28(5):1141–6. doi:10.1007/s10554-011-9929-8. PubMed.
25. Fielden SW, Fornwalt BK, Jerosch-Herold M, Eisner RL, Stillman AE, Oshinski JN. A new method for the determination of aortic pulse wave velocity using cross-correlation on 2D PCMR velocity data. J Magn Reson Imaging. 2008;27(6):1382–7. doi:10.1002/jmri.21387. PubMed.
26. Gatehouse PD, Rolf MP, Graves MJ, Hofman MB, Totman J, Werner B, Quest RA, Lin Y, Von Spiczak J, Dieringer M, Firmin DN, Van Rossum A, Lombardi M, Schwitter J, Schultz-Menger J, Kilner PJ. Flow measurement by cardiovascular magnetic resonance: a multi-centre multi-vendor study of background phase offset errors that can compromise the accuracy of derived regurgitant or shunt flow measurements. J Cardiovasc Magn Reson: Off J Soc Cardiovasc Magn Reson. 2010;12:5. doi:10.1186/1532-429X-12-5. PubMed PMID: 20074359; PubMed Central PMCID: PMC2818657.

27. Gatehouse PD, Keegan J, Crowe LA, Masood S, Mohiaddin RH, Kreitner KF, Firmin DN. Applications of phase-contrast flow and velocity imaging in cardiovascular MRI. Eur Radiol. 2005;15(10):2172–84. doi:10.1007/s00330-005-2829-3. PubMed.
28. Bhatia RS, Tu JV, Lee DS, Austin PC, Fang J, Haouzi A, Gong Y, Liu PP. Outcome of heart failure with preserved ejection fraction in a population-based study. N Engl J Med. 2006;355:260–9.
29. Owan TE, Hodge DO, Herges RM, Jacobsen SJ, Roger VL, Redfield MM. Trends in prevalence and outcome of heart failure with preserved ejection fraction. N Engl J Med. 2006;355:251–9.
30. Bollache E, Redheuil A, Clement-Guinaudeau S, Defrance C, Perdrix L, Ladouceur M, Lefort M, De Cesare A, Herment A, Diebold B, Mousseaux E, Kachenoura N. Automated left ventricular diastolic function evaluation from phase-contrast cardiovascular magnetic resonance and comparison with Doppler echocardiography. J Cardiovasc Magn Reson. 2010;12:63.
31. Rathi VK, Doyle M, Yamrozik J, Williams RB, Caruppannan K, Truman C, Vido D, Biederman RW. Routine evaluation of left ventricular diastolic function by cardiovascular magnetic resonance: a practical approach. J Cardiovasc Magn Reson. 2008;10:36.
32. Hartiala JJ, Mostbeck GH, Foster E, Fujita N, Dulce MC, Chazouilleres AF, Higgins CB. Velocity-encoded cine MRI in the evaluation of left ventricular diastolic function: measurement of mitral valve and pulmonary vein flow velocities and flow volume across the mitral valve. Am Heart J. 1993;125:1054–66.
33. Buss SJ, Krautz B, Schnackenburg B, Abdel-Aty H, Santos MF, Andre F, Maertens MJ, Mereles D, Korosoglou G, Giannitsis E, Katus HA, Steen H. Classification of diastolic function with phase-contrast cardiac magnetic resonance imaging: validation with echocardiography and age-related reference values. Clin Res Cardiol. 2014;103:441–50.
34. Paelinck BP, De Roos A, Bax JJ, Bosmans JM, Van der Geest RJ, Dhondt D, Parizel PM, Vrints CJ, Lamb HJ. Feasibility of tissue magnetic resonance imaging: a pilot study in comparison with tissue Doppler imaging and invasive measurement. J Am Coll Cardiol. 2005;45:1109–16.
35. Gupta A, Singh Gulati G, Seth S, Sharma S. Cardiac MRI in restrictive cardiomyopathy. Clin Radiol. 2012;67:95–105.
36. Bertog SC, Thambidorai SK, Parakh K, Schoenhagen P, Ozduran V, Houghtaling PL, Lytle BW, Blackstone EH, Lauer MS, Klein AL. Constrictive pericarditis: etiology and cause-specific survival after pericardiectomy. J Am Coll Cardiol. 2004;43:1445–52.
37. Talreja DR, Edwards WD, Danielson GK, Schaff HV, Tajik AJ, Tazelaar HD, Breen JF, Oh JK. Constrictive pericarditis in 26 patients with histologically normal pericardial thickness. Circulation. 2003;108:1852–7.
38. O'brien KR, Cowan BR, Jain M, Stewart RA, Kerr AJ, Young AA. MRI phase contrast velocity and flow errors in turbulent stenotic jets. J Magn Reson Imaging. 2008;28:210–8.
39. Sondergaard L, Stahlberg F, Thomsen C. Magnetic resonance imaging of valvular heart disease. J Magn Reson Imaging. 1999;10:627–38.
40. Gelfand EV, Hughes S, Hauser TH, Yeon SB, Goepfert L, Kissinger KV, Rofsky NM, Manning WJ. Severity of mitral and aortic regurgitation as assessed by cardiovascular magnetic resonance: optimizing correlation with Doppler echocardiography. J Cardiovasc Magn Reson. 2006;8:503–7.
41. Kondo C, Caputo GR, Semelka R, Foster E, Shimakawa A, Higgins CB. Right and left ventricular stroke volume measurements with velocity-encoded cine MR imaging: in vitro and in vivo validation. AJR Am J Roentgenol. 1991;157:9–16.
42. Cawley PJ, Hamilton-Craig C, Owens DS, Krieger EV, Strugnell WE, Mitsumori L, D'jang CL, Schwaegler RG, Nguyen KQ, Nguyen B, Maki JH, Otto CM. Prospective comparison of valve regurgitation quantitation by cardiac magnetic resonance imaging and transthoracic echocardiography. Circ Cardiovasc Imaging. 2013;6:48–57.
43. Chatzimavroudis GP, Oshinski JN, Franch RH, Pettigrew RI, Walker PG, Yoganathan AP. Quantification of the aortic regurgitant volume with magnetic resonance phase velocity mapping: a clinical investigation of the importance of imaging slice location. J Heart Valve Dis. 1998;7:94–101.
44. Heidenreich PA, Steffens J, Fujita N, O'sullivan M, Caputo GR, Foster E, Higgins CB. Evaluation of mitral stenosis with velocity-encoded cine-magnetic resonance imaging. Am J Cardiol. 1995;75:365–9.
45. Nishimura RA, Otto CM, Bonow RO, Carabello BA, 3rd Erwin JP, Guyton RA, O'gara PT, Ruiz CE, Skubas NJ, Sorajja P, 3rd Sundt T, Thomas JD. 2014 AHA/ACC guideline for the management of patients with valvular heart disease: executive summary: a report of the American College of Cardiology/American Heart Association Task Force on Practice Guidelines. J Am Coll Cardiol. 2014;63:2438–88.
46. Buchner S, Debl K, Poschenrieder F, Feuerbach S, Riegger GA, Luchner A, Djavidani B. Cardiovascular magnetic resonance for direct assessment of anatomic regurgitant orifice in mitral regurgitation. Circ Cardiovasc Imaging. 2008;1:148–55.
47. Chatzimavroudis GP, Oshinski JN, Pettigrew RI, Walker PG, Franch RH, Yoganathan AP. Quantification of mitral regurgitation with MR phase-velocity mapping using a control volume method. J Magn Reson Imaging. 1998;8:577–82.
48. Botnar R, Nagel E, Scheidegger MB, Pedersen EM, Hess O, Boesiger P. Assessment of prosthetic aortic valve performance by magnetic resonance velocity imaging. MAGMA. 2000;10:18–26.
49. Ribeiro HB, Le Ven F, Larose E, Dahou A, Nombela-Franco L, Urena M, Allende R, Amat-Santos I, Ricapito Mde L, Thebault C, Clavel MA, Delarochelliere R, Doyle D, Dumont E, Dumesnil JG, Pibarot P, Rodes-Cabau J. Cardiac magnetic resonance versus transthoracic echocardiography for the assessment and quantification of aortic regurgitation in patients undergoing transcatheter aortic valve implantation. Heart. 2014;100:1924–32.
50. Oshinski JN, Parks WJ, Markou CP, Bergman HL, Larson BE, Ku DN, Mukundan Jr S, Pettigrew RI. Improved measurement of pressure gradients in aortic coarctation by magnetic resonance imaging. J Am Coll Cardiol. 1996;28:1818–26.
51. Warnes CA. The adult with congenital heart disease: born to be bad? J Am Coll Cardiol. 2005;46(1):1–8.
52. Rajiah P, Kanne JP. Cardiac MRI: part 1, cardiovascular shunts. AJR. 2011;197(4):W603–20.
53. Mercer-Rosa L, Yang W, Kutty S, Rychik J, Fogel M, Goldmuntz E. Quantifying pulmonary regurgitation and right ventricular function in surgically repaired tetralogy of fallot. A comparative analysis of echocardiography and magnetic resonance imaging. Circ Cardiovasc Imaging. 2012;5(5):637–43.
54. Geva T. Repaired tetralogy of Fallot: the roles of cardiovascular magnetic resonance in evaluating pathophysiology and for pulmonary valve replacement decision support. J Cardiovasc Magn Reson. 2011;13:9.
55. Kondo C, Caputo GR, Masui T, Foster E, O'sullivan M, Stulbarg MS, Golden J, Chatterjee K, Higgins CB. Pulmonary hypertension: pulmonary flow quantification and flow profile analysis with velocity-encoded cine MR imaging. Radiology. 1992;183(3):751–8.
56. Sanz J, Kuschnir P, Rius T, Salguero R, Sulica R, Einstein AJ, Dellagrottagle S, Fuster V, Rajagopalan S, Poon M. Pulmonary arterial hypertension: noninvasive detection with phase- contrast MR imaging. Radiology. 2007;243:70–7.
57. Reiter G, Reiter U, Kovacs G, Kainz B, Schmidt K, Maier R, Olschewski H, Rienmueller R. Magnetic resonance-derived 3-dimensional blood flow patterns in the main pulmonary artery as a marker of pulmonary hypertension and a measure of elevated mean pulmonary arterial pressure. Circ Cardiovasc Imaging. 2008;1:23–30.
58. Bradlow WM, Simon J, Gibbs R, Mohiaddin RH. Cardiovascular magnetic resonance in pulmonary hypertension. J Cardiovasc Magn Reson. 2012;14(1):1–12.